Asian Journal of Chemistry; Vol. 29, No. 10 (2017), 2327-2332

ASIAN JOURNAL OF CHEMISTRY

https://doi.org/10.14233/ajchem.2017.20921

Di-μ-oxidovanadium(V) Complex with N'-[(*Z*)-Phenyl(pyridin-2-yl)methylidene]pyridine-4-carbohydrazide: Synthesis, Structural Characterization and *in vitro* Antidiabetic Inhibition Study

R.N. PATEL* and YOGENDRA PRATAP SINGH

Department of Chemistry, A.P.S. University, Rewa-486 003, India

*Corresponding author: E-mail: rnp64@ymail.com

Received: 10 July 2017; *Accepted*: 5 August 2017; *Published online*: 31 August 2017; AJC-18543

Schiff base and its one di-μ-oxidovanadium(V) complex have been synthesized by the reaction of vanadyl sulphate pentahydrate and N'-[(*Z*)-phenyl(pyridin-2-yl)methylidene]pyridine-4-carbohydrazide (HL). The HL and its complex [(L)VO(μ-O)$_2$VO(L)] have been characterized by micro-analysis, UV-visible and electrochemical techniques. The ligand and its complex have also been characterized by single crystal X-ray technique. The ligand crystallizes in triclinic crystal system with $P\bar{1}$ space group while, complex crystallizes in monoclinic crystal system with $P2_1/c$ space group. The electronic spectrum is as expected for vanadium(V) in an octahedral environment in each vanadium centers. The electronic structures of the ligand and the complex have been explained by density functional theory (DFT) calculations. In addition, *in vitro* insulin mimetic activity of the complex has also been evaluated.

Keywords: Hydrazone Schiff base, Vanadium(V) complex, Crystal structures, Electrochemistry, UV-visible spectra.

INTRODUCTION

Vanadium is one of the essential trace elements in animals and humans. Several studies have shown its important role in both glucose and lipid metabolism and in turn to exhibit insulin-mimetic activity [1-6]. Insulin, a pancreatic signaling hormone, is the principal treatment for type 1 diabetes and is often required for type 2 diabetes as well. Insulin is not orally active and must be administered *via* intramuscular injection. Vanadium compounds stimulate glucose metabolism without affecting the concentration of insulin. This makes them promising candidates for the treatment of type 2 diabetic individuals.

Interest in the coordination chemistry of di-μ-oxidovanadium(V) complexes have been motivated by the emphasis on biological and catalytic relevance of such complexes. In this study, we report the synthesis, structural characterization and *in vitro* antidiabetic activity (α-glucosidase inhibition activity). The experimental data also corroborated by DFT calculations. The main goal of DFT calculations was to obtain well converged structural parameters.

EXPERIMENTAL

All the chemicals and solvents were used reagent grade and used further without purification. $VOSO_4 \cdot 5H_2O$ was obtained from S.D. Fine Chemicals.

Elemental analyses were performed on a Euro Vector EA3000 elemental analyzer. X-ray quality single crystals were obtained by slow cooling of methanol solutions containing HL and [(L)VO(μ-O)$_2$VO(L)]. Diffraction data were collected on a Rigaku Oxford Diffraction Gemini Eos, Dual-source auto diffractometer. Data collection and processing was performed using the programs CrysAlisPro [7] and a multi-scan absorption correction was applied using SCALE3 ABSPACK [7]. The structures were solved using direct methods [8], which revealed the position of all non-hydrogen atoms. These atoms were refined on F^2 by a full-matrix least-squares procedure using anisotropic displacement parameters [9]. All hydrogen atoms were located in different Fourier maps and included as fixed positions riding on attached atoms with isotropic thermal displacement parameters 1.2 (C–H, N–H) or 1.5 (O–H) times those of the respective atom. All calculations were performed using PLATON [10] and WinGX [11] programs. Crystallographic data are summarized in Table-1. The CIF files are obtained free of charge from Cambridge Crystallographic Data Center (CCDC) under CCDC number 1561498 and 1561499 contains the supplementary crystallographic data for ligand (HL) and [(L)VO(μ-O)$_2$VO(L)], respectively.

UV-visible spectra (250-600 nm range) were measured in DMSO on a Shimadzu 1601 spectrophotometer. Infrared spectra (4000-400 cm^{-1}) of the solid samples were recorded on a Bruker Alpha-T, FT-IR spectrophotometer. The electrochemistry of the ligand and complex (3×10^{-3} M) in DMSO

TABLE-1
CRYSTAL DATA AND STRUCTURE REFINEMENT PARAMETER FOR HL AND DI-μ-OXIDOVANADIUM(V) COMPLEX

	HL	$[(L)VO(\mu\text{-}O)_2VO(L)]$
Empirical formula	$C_{18}H_{14}N_4O$	$C_{36}H_{26}N_8O_6V_2$
Formula weight	302.33	768.53
Temperature (K)	173(2)	173(2)
Wavelength (Å)	1.54184	1.54184
Crystal system	Triclinic	Monoclinic
Space group	P1	$P2_1/c$
a (Å)	8.1416(7)	14.6449(4)
b (Å)	8.6565(7)	8.2316(2)
c (Å)	11.0864(7)	14.5244(4)
α (°)	91.628(6)	90
β (°)	94.343(6)	110.823(3)
γ (°)	109.672(7)	90
Volume ($Å^3$)	732.42(10)	1636.56(8)
Z	2	2
Density (calcd.) (Mg/m^3)	1.371	1.560
Absorption coeff. (mm^{-1})	0.716	5.311
Crystal size (mm^3)	0.46 × 0.39 × 0.17	0.49 × 0.35 × 0.15
θ (°)	4.006 to 71.532	3.229 to 71.421
Index ranges	$-9 \le h \le 10$, $-10 \le k \le 9$, $-7 \le l \le 13$	$-17 \le h \le 16$, $-7 \le k \le 9$, $-17 \le l \le 17$
Goodness-of-fit on F^2	1.024	1.046
Data/restraints/parameters	2764/0/209	3099/0/235
Final R indices [I>2σ(I)]	R1 = 0.0391, wR2 = 0.1050	R1 = 0.0475, wR2 = 0.1254
R indices (all data)	R1 = 0.0423, wR2 = 0.1078	R1 = 0.0534, wR2 = 0.1333

containing 0.1 M tetra-butylammonium perchlorate (TBAP) as a supporting electrolyte was determined at room temperature by cyclic voltammetry (CV) using a three-electrode system under nitrogen atmosphere conditions on a BAS 100 electrochemical analyzer. A glassy-carbon and platinum wire was used as the working electrode and the counter electrode, respectively. The reversibility of the electrochemical process was evaluated by standard procedures and all potentials were recorded against a Ag/AgCl reference electrode. All measurements were carried out at 298 K under nitrogen atmosphere. Method for determination of α-glucosidase inhibition study was adopted as reported in the literature [5,12]. All the computational calculations were performed with GAUSSIAN09 program package [13] with the aid of the Gauss View05 visualization program.

Synthesis of ligand [HL]: It was prepared following the procedure previously reported [14]. A solution of benzoylhydrazine (0.681 g, 5 mmol) and 2-benzoylpyridine (0.916 g, 5 mmol) were refluxed for 6 h in 25 mL ethanol and cooled to room temperature. The product formed was filtered off and washed with ethanol to obtain a pale yellow crystalline compound. Yield about 87 %. Anal. calcd. for ($C_{18}H_{14}N_4O$) (m.w. = 302.33 g mol^{-1}) Anal.: C, 71.48; H, 4.61; N, 18.51 %. Calcd.: C, 71.51; H, 4.67; N, 18.53; O, 5.29 %.

Synthesis of $[(L)VO(\mu\text{-}O)_2VO(L)]$: Aqueous solution of 15 mL of $VOSO_4 \cdot 5H_2O$ (0.506 g, 2 mmol) was added to solution of HL (0.604 g, 2 mmol) dissolved in 40 mL of methanol and the resulting reaction mixture was refluxed for 3 h. This solution was cooled and left at room temperature for about 24 h, it resulted in the separation of light yellow crystalline solid. This was filtered off washed with methanol and dried in $CaCl_2$ desiccators. Yield: ~ 62 %. Anal. calcd. for ($C_{36}H_{26}N_8O_6V_2$) (M = 768.53 g mol^{-1}) Anal.: C, 56.29; H, 3.39; N, 14.54 %. Calcd.: C, 56.26; H, 3.41; N, 14.58; O, 12.49; V, 13.26 %. Electronic absorption spectrum in DMSO [$\lambda_{max.}$, nm (ε, M^{-1} cm^{-1})]: 311 (379), 401 (673).

RESULTS AND DISCUSSION

Synthesis and characterization: N'-[(*Z*)-Phenyl(pyridin-2-yl)methylidene]pyridine-4-carbohydrazide (HL) was prepared from the condensation reaction between 2-benzoylpyridine and hydrazide in ethanol medium. The ligand was obtained with sufficient purity and used without further purification in the synthesis of complex. The reaction of ligand (HL) and vanadyl sulphate in methanol gave to complexes $[(L)VO(\mu\text{-}O)_2VO(L)]$. The ligand (HL) and its complex $[(L)VO(\mu\text{-}O)_2VO(L)]$ are stable in air and were characterized by physical methods such as microanalysis, IR spectra and further characterized by single crystal X-ray crystallography.

IR spectral studies: The ligand shows bands at 1615 cm^{-1} for HL. This bands shift toward lower wave numbers on complexation, indicating complexation of azomethine nitrogen to the vanadium [14]. The IR spectra of ligand show a sharp band about 1675 cm^{-1} due to ν(C=O) of the hydrazide moiety. The absence of this band in complexes indicates that their enolization and replacement. In addition, complex show one sharp band at about 940 cm^{-1} and a bro ad band at about 860 cm^{-1} assigned to ν[V-(μ-O)-V] [14,15].

Electronic spectral studies: Electronic spectra of the ligand (HL) and complex were recorded in DMSO solutions and are shown in Fig. 1. UV spectra of the ligand show five sharp bands in the range 250-600 nm. The probable assignment of the first two bands is $\phi \rightarrow \phi^*$ and $\pi \rightarrow \pi^*$, while the last band is assignable to a $\pi \rightarrow \pi^*$ transition. Assignment of the remaining intra-ligand bands was not possible. On coordination, the $\phi \rightarrow \phi^*$ and $\pi \rightarrow \pi^*$ transitions move toward higher wavelengths while the $n \rightarrow \pi^*$ transition merges with an additional broad band due to ligand-to-metal charge transfer (MLCT) from an alkoxide oxygen to an empty *d*-orbital of this metal [16-18]. As vanadium(V) complex have a $3d^0$ configuration, the *d-d* bands are not expected for the present complex. Only two bands in the

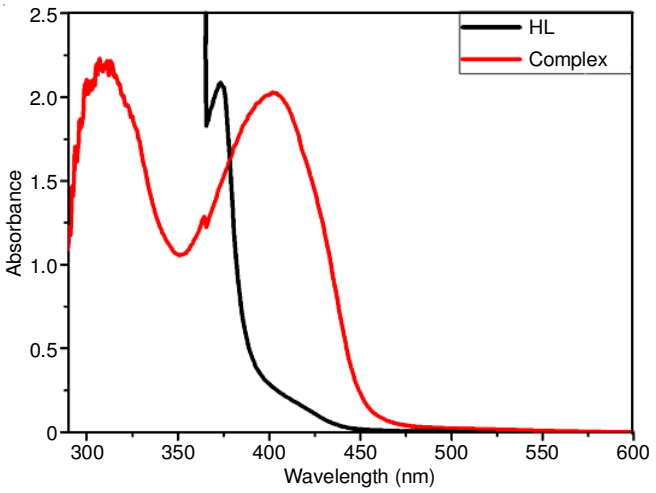

Fig. 1. UV-visible spectra of ligand HL and $[(L)VO(\mu\text{-}O)_2VO(L)]$ in DMSO solution (3.0×10^{-3} M)

UV-region (301/299 nm) form $\phi \rightarrow \phi^*$ transitions and 405/413 nm for $\pi \rightarrow \pi^*$ transitions as shown in Fig. 1 [17,18]. In these complexes *d-d* bands are not observed for vanadium(V) [18].

Molecular structures of ligand and complex: An ORTEP view of HL is shown in Fig. 2. The main bond angles and distances are presented in Table-2. HL crystallized in the triclinic, $P\bar{1}$ space group. The configuration of the ligand in the solid state is illustrated for its coordination with the metal as an NNO donor, mononegative tridentate chelate. The distances of N2–C6 = 1.2951(16) Å, O1-C13 = 1.2183(15) and N2-N3 = 1.3669(14) Å are close to those theoretically predicted for a C=N double bond (1.28 Å), C=O double bond (1.22 Å) and N=N double bond (1.35 Å), respectively, confirming formation of a Schiff base. The bond angle of O(1)–C13–C(14) is 121.77° which is consistent with the calculated value of 120.1° and similar to other complexes reported in the literature [19]. In the hydrazone linkage, the angle for C(13)-N(3)-N(2) was calculated 125.23°, whereas, the observed value is 120.33°. This is similar to the values reported in the literature [20,21]. The carbonyl moiety makes an angle with the hydrazone moiety of 124.98(11)°, which is slightly different from the calculated value 128.26°. The conformation of the ligand molecule is mainly determined by the intermolecular hydrogen bond between the hydrazone nitrogen atom N(3) and pyridine nitrogen atom N(1), N(3)-H(3B)···N(1) = 2.6180(14) Å (Table-3). The free ligand HL remains in its keto tautomeric form with the keto oxygen atom and *cis* to the azomethine nitrogen atom. The bond N(2)-N(3) behaves as bridge between the benzoyl pyridine and benzoyl ring [22,23]. A comparison of the N(2)-N(3) distance of 1.3669(14) Å with that in benzoyl hydrazide shows that the bond is shorter than a single N-N bond

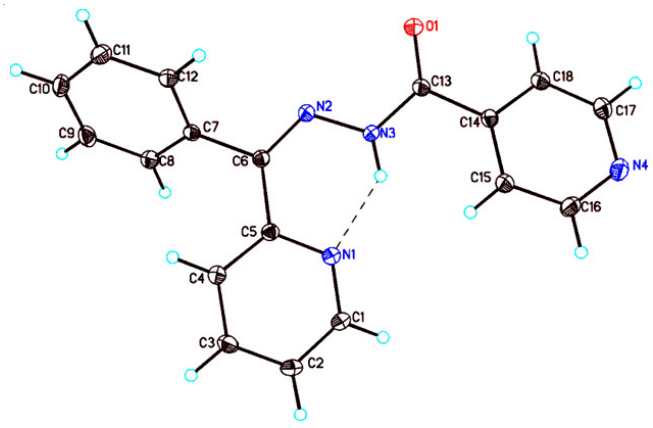

Fig. 2. Molecular structure of Schiff base HL, showing the atom labelling system and 30 % thermal ellipsoids

TABLE-2
SELECTED INTER ATOMIC DISTANCES (Å) AND BOND ANGLES (°) FOR SCHIFF BASE (HL)

Bond distances			
O(1)-C(13)	1.2183(15)	N(4)-C(17)	1.3368(18)
N(1)-C(1)	1.3379(16)	N(4)-C(16)	1.3411(18)
N(1)-C(5)	1.3519(15)	C(1)-C(2)	1.3838(18)
N(2)-C(6)	1.2951(16)	C(2)-C(3)	1.3781(18)
N(2)-N(3)	1.3669(14)	C(3)-C(4)	1.3857(18)
N(3)-C(13)	1.3617(16)	C(4)-C(5)	1.3932(17)
C(5)-C(6)	1.4934(16)	C(6)-C(7)	1.4928(16)
Bond angles			
C(1)-N(1)-C(5)	118.40(10)	C(6)-N(2)-N(3)	117.72(10)
C(13)-N(3)-N(2)	120.33(10)	N(1)-C(1)-C(2)	123.83(12)
C(17)-N(4)-C(16)	116.60(11)	C(3)-C(2)-C(1)	117.72(11)
C(2)-C(3)-C(4)	119.56(12)	C(3)-C(4)-C(5)	119.49(12)
N(1)-C(5)-C(4)	120.99(11)	N(1)-C(5)-C(6)	117.80(10)
C(4)-C(5)-C(6)	121.17(11)	N(2)-C(6)-C(7)	114.49(10)
N(2)-C(6)-C(5)	127.74(11)	C(7)-C(6)-C(5)	117.70(10)
C(12)-C(7)-C(8)	118.79(11)	C(12)-C(7)-C(6)	120.00(11)
C(8)-C(7)-C(6)	121.21(11)	C(9)-C(8)-C(7)	120.34(12)
C(10)-C(9)-C(8)	120.27(12)	C(9)-C(10)-C(11)	119.89(12)
C(12)-C(11)-C(10)	120.05(12)	C(11)-C(12)-C(7)	120.59(12)
O(1)-C(13)-N(3)	124.98(11)	O(1)-C(13)-C(14)	121.77(11)
N(3)-C(13)-C(14)	113.25(10)	C(18)-C(14)-C(15)	117.76(11)
C(18)-C(14)-C(13)	118.00(11)	C(15)-C(14)-C(13)	124.25(11)
C(16)-C(15)-C(14)	119.03(12)	N(4)-C(16)-C(15)	123.65(12)
N(4)-C(17)-C(18)	124.06(12)	C(17)-C(18)-C(14)	118.88(12)

(1.40 Å) indicating that a significant π-charge delocalization occurs along the C-N-N-C moiety. A remarkable feature of the crystal structure of HL is formation of inter and intramolecular H-bonding through the azo nitrogen, amide nitrogen (NH), pyridine nitrogen (N) and ketonic (O) of hydrazone. The ligand forms hydrogen-bonded chains which run parallel to the *b* and *c* axes creating a 2D supramolecular structure.

The crystal structure of complex has been determined by single crystal X-ray crystallography at 173(2). The molecular structure of the complex along with atom numbering schemes is given in Fig. 3. Bond length and angles are given in Table-4. In the present vanadyl complex the asymmetric unit is formed by one-half of the molecule and the other half is related by a center of inversion. In this complex, the central vanadium atoms are bridged by two oxido oxygen atoms, forming the central V_2O_2 core (Fig. 3). The complex has a $V^V O_4N_2$ psedooctahedral geometry with the V=O distance of 1.6142 Å, indicative of vanadium-oxygen double bond and are commonly in the range from 1.57-1.62 Å [24,25]. The structure of vanadyl complex show that each V^V-center is hexa coordinated in distorted octahedral geometry, with terminal oxygen atom O(1) with symmetry transformations (#1 –x, -y+1, -z+1) used to generate

TABLE-3
HYDROGEN BONDS INTERACTIONS FOR HL AND [(L)VO(μ-O)$_2$VO(L)] (Å AND °)

D–H···A	d(D-H)	d(H···A)	d(D···A)	∠(DHA)	Symmetry transformations
HL					
N(3)-H(3B)...N(1)	0.88	1.91	2.6180(14)	135.7	
C(1)-H(1A)...O(1)#1	0.95	2.60	3.2156(15)	122.7	#1 x, y+1, z
C(2)-H(2A)...O(1)#1	0.95	2.60	3.1955(16)	121.0	#1 x, y+1, z
C(2)-H(2A)...N(2)#1	0.95	2.63	3.5735(16)	174.5	#1 x, y+1, z
[(L)VO(μ-O)$_2$VO(L)]					
C(2)-H(2A)...O(1)#2	0.95	2.62	3.197(3)	119.9	#2 -x, y+1/2, -z+3/2
C(17)-H(17A)...O(2)#3	0.95	2.55	3.377(3)	145.6	#3 -x, -y, -z+1

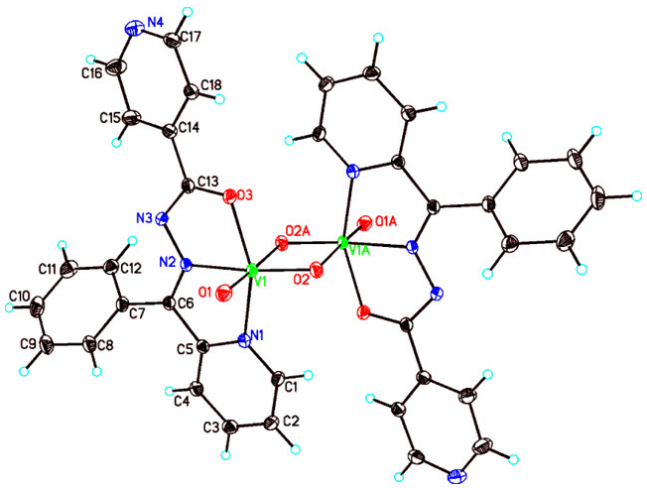

Fig. 3. Molecular structure of [(L)VO(μ-O)$_2$VO(L)], showing the atom labelling system and 30 % thermal ellipsoids

equivalent atoms. O(1A) are strongly bonded to V(1A) [V(1)-O(1A) = 1.6142 (19) Å] (Table-4) [25]. O(2A) is weakly associated with V(1) [V(1)-O(1A) #1 = 2.3513 (19) Å (Table-4 and Fig. 3). The remaining three coordination sites are occupied by the pyridine N atom [V(1)-N(1) = 2.114(2) Å], azomethine N atom [V(1)-N(2) = 2.124(2) Å] and ketonic O atom [V(1)-O(3) = 1.9732(18) Å]. The V-V distance is V(1)-V(1A) = 3.142 Å and globally the O-V-O and V-O-V angles are 78.38° and 101.62°, respectively similar to those observed in other similar complexes [14,25]. Oxygen atom of V=O and bridging oxygen atom are responsible for a hydrogen bond interactions.

TABLE-4
SELECTED INTER ATOMIC DISTANCES (Å) AND BOND ANGLES (°) FOR COMPLEX [(L)VO(μ-O)$_2$VO(L)]

Bond distances			
V(1)-O(1)	1.6142(19)	V(1)-O(2)	1.6634(18)
V(1)-O(3)	1.9732(18)	V(1)-N(1)	2.114(2)
V(1)-N(2)	2.124(2)	V(1)-O(2)#1	2.3513(19)
O(2)-V(1)#1	2.3513(19)		
Bond angles			
O(1)-V(1)-O(2)	106.91(10)	O(1)-V(1)-O(3)	99.10(9)
O(2)-V(1)-O(3)	105.17(8)	O(1)-V(1)-N(1)	93.46(9)
O(2)-V(1)-N(1)	100.27(9)	O(3)-V(1)-N(1)	146.79(8)
O(1)-V(1)-N(2)	98.94(9)	O(2)-V(1)-N(2)	153.73(9)
O(3)-V(1)-N(2)	74.64(8)	N(1)-V(1)-N(2)	73.09(8)
O(1)-V(1)-O(2)#1	174.26(9)	O(2)-V(1)-O(2)#1	78.38(9)
O(3)-V(1)-O(2)#1	81.36(7)	N(1)-V(1)-O(2)#1	83.26(7)
N(2)-V(1)-O(2)#1	75.62(7)	V(1)-O(2)-V(1)#1	101.62(9)

Symmetry transformations used to generate equivalent atoms:
#1 -x,-y+1,-z+1

Tetragonality parameter: In hexa-coordinated metal(II) complexes, the degree of structural distortion from ideal octahedral geometry can be ascertained through a tetragonality parameter defined as: $T = R_{int}/R_{out}$, where R_{int} and R_{out} are the average in-plane and out-of-plane distances, respectively. Distortion in solid state and in solution state showing tetragonality at relatively higher temperature is referred as static Jahn-Teller effect and distortion not showing or small due to random movement of bonds which does not allow the measurement within a time frame is referred as dynamic Jahn-Teller effect. The behaviour of Jahn-Teller effect is decided by the calculated T values of vanadyl complex. This parameter indicates static ($T < 0.9$) and dynamic ($T = 1$) distortions in molecular geometry [26,27]. For the present vanadyl complex, T value (1.063) showing a dynamic Jahn-Teller effect.

Electrochemistry: The electrochemical behaviour of HL and its complex was studied using cyclic voltammetry (CV). Cyclic voltammograms of the samples are shown in Fig. 4. In Fig. 4 the HL showed no electrochemical response in the range of -0.1 to -1.0 V. The electrochemical behaviour of this complex is believed to be due to the vanadium(V)→vanadium(IV) couples. Two distinct reduction peaks at -0.622 V and -0.804 V were seen for this homobinuclear vanadium(V) complexes. In an initial anodic scan CV does not yield any oxidation peaks. The reduction process may involve the following electron-transfer reactions [25]:

$$V^{V}\ V^{V} \xrightarrow{+e^-} V^{IV}\ V^{V} \xrightarrow{+e^-} V^{IV}\ V^{IV}$$

Electron transfer reaction waves of HL and complex were also studied by differential pulse voltammetry (DPV). DPV measurements yielded similar observations where the potential

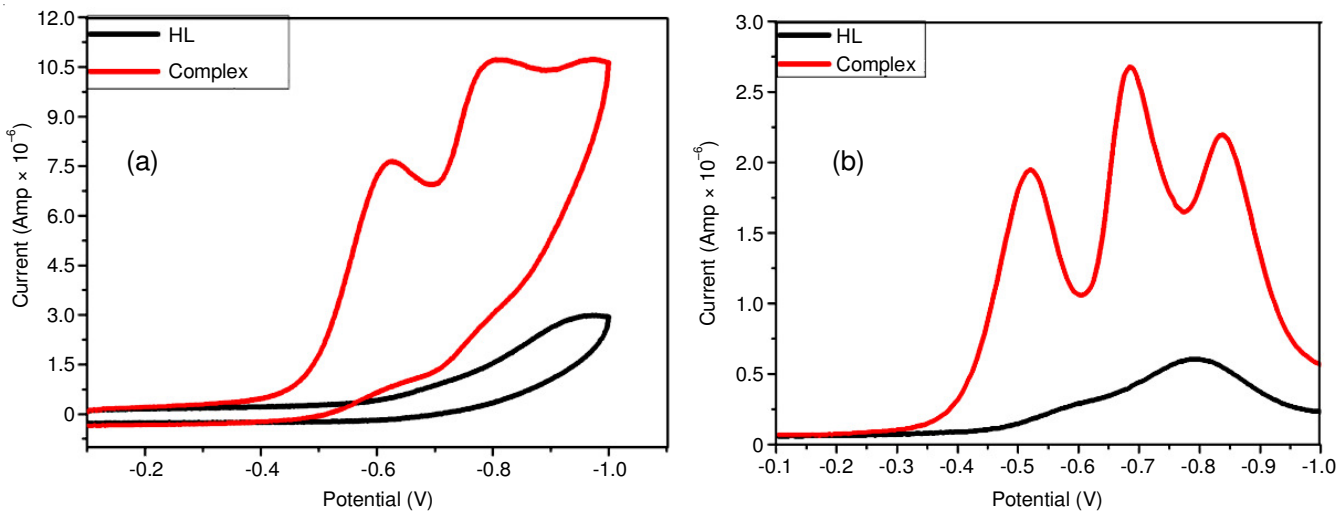

Fig. 4. (a) Cycle voltammograms of HL and [(L)VO(μ-O)$_2$VO(L)] in DMSO at an Ag/AgCl electrode with scan rate 300 mV s^{-1} and temperature 20 °C, (b) Differential pulse voltammogram of HL and [(L)VO(μ-O)$_2$VO(L)] at room temperature using a scan rate 20 mV s^{-1} in DMSO. The pulse amplitude is 50 mV

(E_{pc} = -0.784 V for HL and E_{pc}^{1} = -0.524 V, E_{pc}^{2} = -0.680 V and E_{pc}^{3} = -0.832 V for complex) agreed with those measured by other electrochemical methods. In DPV, one extra peak potential was observed which correspond to reduction of ligand moiety. These electrochemical techniques also helped to establish the homobinuclear vanadium(V) complex [28].

Electronic structure DFT calculations: The coordinates obtained from single crystal X-ray diffraction data for synthesized Schiff base HL and vanadyl complex were optimized using the DFT/UB3LYP(LANL2DZ/631G(d)) level of calculations. The optimized structures of HL and its complex are shown in Fig. 5 and optimized bond length and angles are well correlated with X-ray data (Tables 2 and 4). According to Tables 2 and 4, the optimized bond lengths and angles are slightly larger than the experimental ones since the theoretical calculations were performed on isolated molecules in gas phase, whereas the experimental results were obtained in solid state [29]. Counter plots of HOMO, LUMO molecular orbitals of HL and complex are shown in Fig. 6. For complex, highest occupied molecular orbital (HOMO) are concentrated on the ligand (100 %) of α-spin

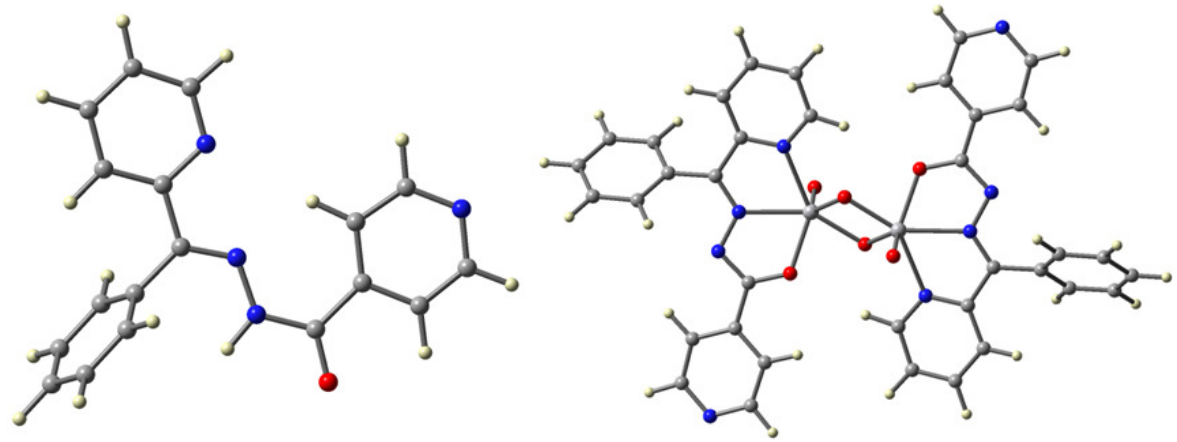

Fig. 5. DFT calculated optimized structure of HL and [(L)VO(μ-O)$_2$VO(L)]

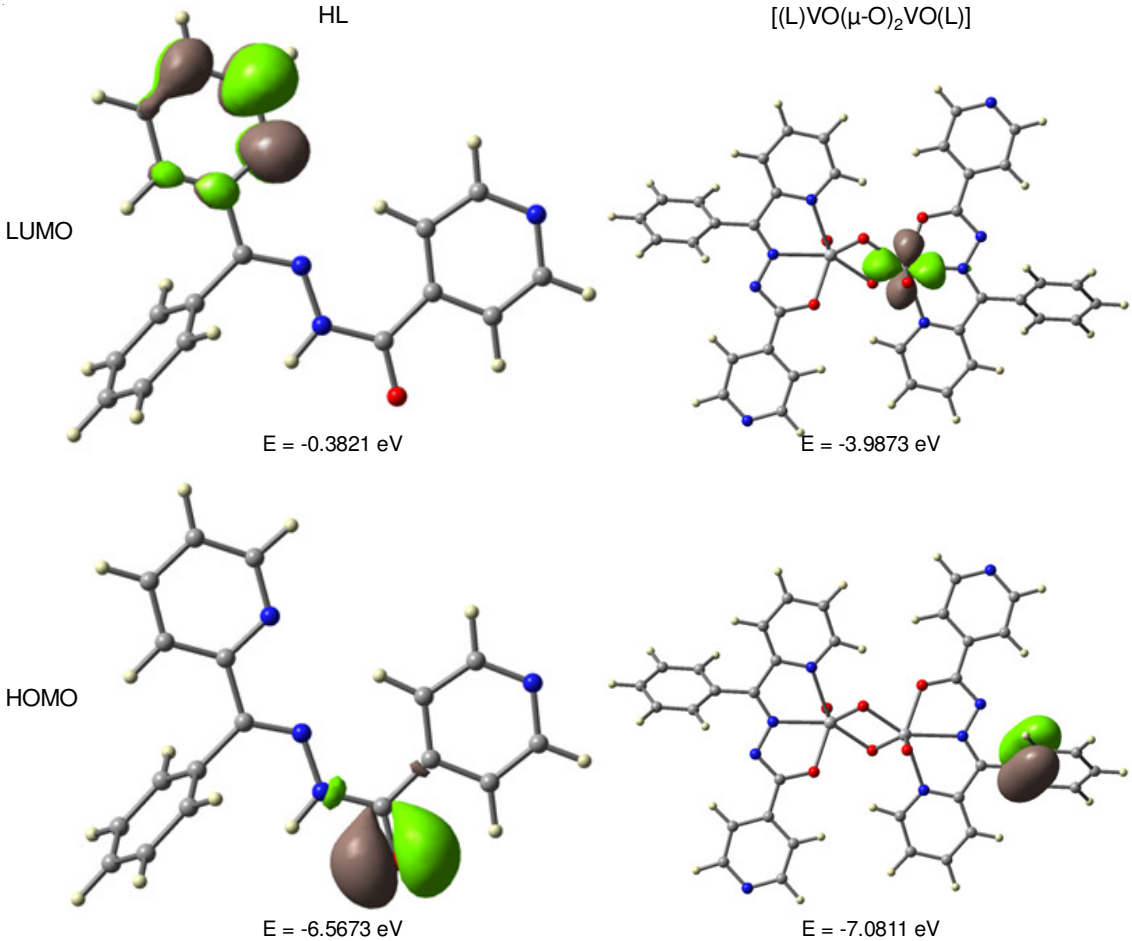

Fig. 6. HOMO and LUMO molecular orbital of HL and [(L)VO(μ-O)$_2$VO(L)]

state. The α-spin unoccupied molecular orbital has 100 % metal $d_{x^2-y^2}$ and d_{z^2} character with reduced contribution from ligand. The LUMO orbitals of HL and complex exhibit a large number of nodes than HOMO orbitals.

***in vitro* insuline-mimitic activity of complex:** Percentage inhibition (α-glucosidase inhibition) data for the complex have been evaluated. From the results, the inhibitory effect of the 200 µg of complex was evaluated by IC_{50} value, which expresses the 50 % inhibition concentration of the complex on α-glucosidase. Thus, the IC_{50} value of the complex was estimated to be 42 µg. This value is similar value for other vanadium complexes [5,30].

Conclusion

The di-µ-oxidovanadium(V) complex with designed Schiff base (HL) has been synthesized and characterized with the aim to investigate the antidiabetic activity of the complex. The molecular structures of HL and its complex have been confirmed by single crystal X-ray studies. The geometrical parameters obtained by DFT calculations are in agreement with XRD results. The complex exhibited two waves, which corresponds to V^V V^V/V^V V^{IV} and V^V V^{IV}/V^{IV} V^{IV} redox processes. Differential pulse voltammetry (DPV) experiments also exhibited the same electrochemical behaviour. DFT calculated bond lengths and angles are in good agreement with the X-ray results. The *in vitro* antidiabetic mimic activity showed that the complex is potent antidiabetic agent.

ACKNOWLEDGEMENTS

Financial assistance from MP Council of Science & Technology, Bhopal, India [Scheme No. A/RD/RP-2/2015-16/245] and SAIF, Central Drug Research Institute, Lucknow, India for providing analytical and spectral facilities are thankfully acknowledged.

REFERENCES

1. Y. Shechter and S.J.D. Karlish, *Nature*, **284**, 556 (1980); https://doi.org/10.1038/284556a0.
2. G.R. Dubyyak and A. Kleinzeller, *J. Biochem.*, **225**, 5306 (1980).
3. C.E. Heyliger, A.G. Tahiliani and J.H. McNeill, *Science*, **227**, 1474 (1985); https://doi.org/10.1126/science.3156405.
4. J. Meyerovitch, Z. Farfel, J. Sack and Y. Shechter, *J. Biochem.*, **262**, 6658 (1987).
5. R.N. Patel, K. Maurya, Y.P. Singh, Y. Singh, S. Rather, A. Kamal and I.P. Tripathi, *J. Indian Chem. Soc.*, **94**, 347 (2017).
6. V. Badmaev, S. Prakash and M. Majeed, *J. Altern. Complement. Med.*, **5**, 273 (1999); https://doi.org/10.1089/acm.1999.5.273.
7. CrysAlisPro, Agilent Technologies, Version 1.171.37.35 (release 13-08-2014 CrysAlis171.NET) (compiled Aug 13 2014, 18:06:01) Empirical Absorption Correction using Spherical Harmonics, Implemented in SCALE3 ABSPACK Scaling Algorithm.
8. G.M. Sheldrick, *Acta Crystallogr. A*, **64**, 112 (2008); https://doi.org/10.1107/S0108767307043930.
9. G.M. Sheldrick, *Acta Crystallogr. C*, **71**, 3 (2015); https://doi.org/10.1107/S2053229614024218.
10. A.L. Spek, *Acta Crystallogr. D Biol. Crystallogr.*, **65**, 148 (2009); https://doi.org/10.1107/S090744490804362X.
11. L.J. Farrugia, *J. Appl. Cryst.*, **45**, 849 (2012); https://doi.org/10.1107/S0021889812029111.
12. S. Mishra, K.B. Pandeya, A.K. Tiwari, A.Z. Ali and T. Saradamani, *J. Indian Chem. Soc.*, **88**, 1195 (2011).
13. M.J. Frisch, G.W. Trucks, H.B. Schlegel, G.E. Scuseria, M.A. Robb, J.R. Cheeseman, G. Scalmani, V. Barone, B. Mennucci, G.A. Petersson, H. Nakatsuji, M. Caricato, X. Li, H.P. Hratchian, A.F. Izmaylov, J. Bloino, G. Zheng, J.L. Sonnenberg, M. Hada, M. Ehara, K. Toyota, R. Fukuda, J. Hasegawa, M. Ishida, T. Nakajima, Y. Honda, O. Kitao, H. Nakai, T. Vreven, J.A. Montgomery Jr., J.E. Peralta, F. Ogliaro, M. Bearpark, J.J. Heyd, E. Brothers, K.N. Kudin, V.N. Staroverov, R. Kobayashi, J. Normand, K. Raghavachari, A. Rendell, J.C. Burant, S.S. Iyengar, J. Tomasi, M. Cossi, N. Rega, J.M. Millam, M. Klene, J.E. Knox, J.B. Cross, V. Bakken, C. Adamo, J. Jaramillo, R. Gomperts, R.E. Stratmann, O. Yazyev, A.J. Austin, R. Cammi, C. Pomelli, J.W. Ochterski, R.L. Martin, K. Morokuma, V.G. Zakrzewski, G.A. Voth, P. Salvador, J.J. Dannenberg, S. Dapprich, A.D. Daniels, O. Farkas, J.B. Foresman, J.V. Ortiz, J. Cioslowski, D.J. Fox, Gaussian Inc., Wallingford CT, Gaussian 09, Revision D.01 (2009).
14. M.R. Maurya, N. Chaudhary, F. Avecilla, P. Adão and J.C. Pessoa, *Dalton Trans.*, **44**, 1211 (2015); https://doi.org/10.1039/C4DT02474E.
15. M.R. Maurya, C. Haldar, A. Kumar, M.L. Kuznetsov, F. Avecilla and J.C. Pessoa, *Dalton Trans.*, **42**, 11941 (2013); https://doi.org/10.1039/c3dt50469g.
16. M.J. Clague, N.L. Keder and A. Butler, *Inorg. Chem.*, **32**, 4754 (1993); https://doi.org/10.1021/ic00074a017.
17. C.J. Carrano, M. Mohan, S.M. Holmes, R. de la Rosa, A. Butler, J.M. Charnock and C.D. Garner, *Inorg. Chem.*, **33**, 646 (1994); https://doi.org/10.1021/ic00082a007.
18. J.M. Arber, E. De Boer, C.D. Garner, S.S. Hasnain and R. Wever, *Biochemistry*, **28**, 7968 (1989); https://doi.org/10.1021/bi00445a062.
19. R.G. Bhirud and T.S. Srivastava, *Inorg. Chim. Acta*, **173**, 121 (1990); https://doi.org/10.1016/S0020-1693(00)91063-6.
20. A. Datta, S.C. Sheu, P.H. Liu and J.H. Huang, *Acta Crystallogr.*, **E67**, m1852 (2011); https://doi.org/10.1107/S1600536811049671.
21. R. Bikas, F. Sattari and B. Notash, *Acta Crystallogr.*, **E68**, 132 (2012); https://doi.org/10.1107/S1600536811055772.
22. H.H. Rassem, A. Salhin, B. Bin Salleh, M.M. Rosli and H.-K. Fun, *Acta Crystallogr.*, **E68**, 1832 (2012); https://doi.org/10.1107/S1600536812021952.
23. H. Kargar, R. Kia and M.N. Tahir, *Acta Crystallogr.*, **E68**, 2321 (2012); https://doi.org/10.1107/S1600536812026633.
24. M.R. Maurya, S. Agarwal, M. Abid, A. Azam, C. Bader, M. Ebel and D. Rehder, *Dalton Trans.*, 937 (2006); https://doi.org/10.1039/B512326G.
25. R.N. Patel, Y.P. Singh, Y. Singh, R.J. Butcher and J.P. Jasinski, *Polyhedron*, **133**, 102 (2017); https://doi.org/10.1016/j.poly.2017.05.028.
26. N. Khadir, D.M. Boghaei, A. Assoud, O.R. Nascimento, A. Nicotina, L. Ghivelder and R. Calvo, *Dalton Trans.*, **44**, 2431 (2015); https://doi.org/10.1039/C4DT03322A.
27. Z.D. Matovic, V.D. Miletic, M. Cendic, A. Meetsma, P.J. van Koningsbruggen and R.J. Deeth, *Inorg. Chem.*, **52**, 1238 (2013); https://doi.org/10.1021/ic301609t.
28. Y.P. Singh, R.N. Patel, Y. Singh, D. Choquesillo-Lazarte and R.J. Butcher, *Dalton Trans.*, **46**, 2803 (2017); https://doi.org/10.1039/C6DT04661D.
29. R.N. Patel, Y.P. Singh, Y. Singh, R.J. Butcher, M. Zeller, R.K.B. Singh and O. U-wang, *J. Mol. Struct.*, **1136**, 157 (2017); https://doi.org/10.1016/j.molstruc.2017.01.083.
30. S. Mishra, K.B. Pandeya, A.K. Tiwari, A.Z. Ali, T. Saradamani, S.B. Agawane and K. Madhusudana, *Int. J. Nutr. Metab.*, **4**, 11 (2012); https://doi.org/10.5897/IJNAM11.045.